

Received March 11, 2020, accepted March 26, 2020, date of publication April 3, 2020, date of current version April 28, 2020.

Digital Object Identifier 10.1109/ACCESS.2020.2985419

Temporally Coordinated Energy Management for AC/DC Hybrid Microgrid Considering Dynamic Conversion Efficiency of Bidirectional AC/DC Converter

BIN WEI¹, (Member, IEEE), XIAOQING HAN¹, (Member, IEEE), PENG WANG², (Fellow, IEEE), HAO YU¹, WEN LI¹, AND LINGJUAN GUO¹

¹School of Electrical and Power Engineering, Taiyuan University of Technology, Taiyuan 030024, China

²School of Electrical and Electronic Engineering, Nanyang Technological University, Singapore 639798

Corresponding author: Xiaqing Han (hanxiaqing@tyut.edu.cn)


This work was supported in part by the National Natural Science Foundation of China under Grant 51777132, and in part by the Major Science and Technology Projects of Shanxi Province under Grant 20181102028.

ABSTRACT Multiple uncertainties from renewable energy sources, power loads and bidirectional AC/DC converter have brought great challenges to the energy management of AC/DC hybrid microgrid. In view of the issues, this paper proposes a temporally coordinated energy management strategy for AC/DC hybrid microgrid considering dynamic conversion efficiency of bidirectional AC/DC converter. According to the operation and loss characteristics of bidirectional AC/DC converter, a novel dynamic conversion efficiency model of bidirectional AC/DC converter is developed. To maintain high robustness at minimum operation cost, the proposed strategy is divided into two stages. The outputs of renewable energy sources, operation characteristics of microgrid components and time-of-use electricity price are comprehensively considered in the day-ahead economic energy management stage to minimize the daily operation cost. In the intraday rolling energy management stage, day-ahead schedules of controllable units are adjusted based on intraday ultra-short-term forecast data to suppress the intraday power fluctuations induced by day-ahead forecast errors. The simulation results demonstrate that the proposed strategy can effectively mitigate the impact of multiple uncertainties and realize the economic operation of AC/DC hybrid microgrid.

INDEX TERMS AC/DC hybrid microgrid, bidirectional AC/DC converter, dynamic conversion efficiency, energy management.

I. INTRODUCTION

Microgrid is a small-scale power generation and distribution system that integrates distribution generators (DGs), energy storages (ESs) and loads [1], [2]. It's an effective carrier for large-scale distributed renewable energy sources (RESs) connected to the existing power grid [3]. Due to natural conditions, the outputs of RESs are intermittent and stochastic [4]. And the load demands are also mainly determined by human behaviors, which are difficult to forecast accurately. These factors have imposed great challenges on the energy management of microgrid [5]–[7].

The associate editor coordinating the review of this manuscript and approving it for publication was Amjad Anvari-Moghaddam .

In recent years, a significant amount of research work has been conducted to investigate the microgrid energy management by the researchers [8]. At present, the microgrid energy management strategy can be mainly categorized into stochastic optimization and robust optimization [9]. According to the literatures, stochastic optimization describes the uncertain information by random variables, and establishes stochastic optimization model by means of probability statistics and stochastic analysis to acquire the minimum cost scheduling [10]–[14]. However, stochastic programming relies too much on the accurate probability curves for different scenarios. In some cases, the model is not accurate enough to reflect the actual situation. Moreover, as the number of scenarios increases, higher computational requirements will be required [15]. In contrast, robust optimization replaces

the accurate probability distribution of random variables with uncertain sets and obtains the optimal scheduling in the worst-case scenario [16]–[19]. Nevertheless, due to the excessive pursuit of the stable operation, the robust optimization often results in over-conservative scheduling [20].

Furthermore, both stochastic optimization and robust optimization are one-time offline optimizations, the intraday fluctuations of RESs and loads are ignored [21]. In view of this issue, multi-time scale optimization has been put forward. Bao *et al.* developed a multi-time scale scheduling for an integrated microgrid. The schedule achieved an integrated optimization for multi energy-type supply and made the microgrid be controllable as seen from the main grid [22]. In [23], an energy management system based on a rolling horizon strategy for a renewable-based microgrid was proposed. For each decision step, a mixed integer optimization problem based on two-day-ahead forecast models was solved. In [24], a temporally-coordinated operation method for a multi-energy microgrid under diverse is proposed considering distinct properties of thermal and power energy. The day-ahead operation makes initial decisions, and online operation replies on a recourse action to compensate day-ahead decisions. Abovementioned works have demonstrated that since longer-time-ahead schedule and real-time operation are both considered in multi-time scale optimization, the source-load uncertainties can be efficiently combat without increasing computational burden.

At present, previous researches of microgrid energy management mainly focused on AC microgrid [25]. In recent years, as the number of DC sources and loads increases, power electronics based rectifiers and inverters in AC microgrid are growing [26]. This not only affects the power quality of microgrid, but also reduces the economy of microgrid operation [27]. AC/DC hybrid microgrid separates AC region from DC region by bidirectional AC/DC converter (BC) and eliminates numerous AC/DC conversions, which effectively solves the above problems [28]. However, in terms of the energy management, the main challenge of traditional AC microgrid is combating the source-load uncertainties. But for the AC/DC hybrid microgrid, the uncertainties both exist in the AC and DC regions. Some literatures also have investigated the energy management of AC/DC hybrid microgrid. Papari *et al.* developed a stochastic framework for the optimal operation of AC/DC hybrid microgrid. A modified crow search algorithm is devised to improve search ability in the problem space [29]. In [30], a bi-level two-stage robust optimal scheduling model for AC/DC hybrid multi-microgrids is proposed in consideration of uncertainties in the utility and supply levels. The model ensured the stable operation of AC/DC hybrid multi-microgrids and achieved the scheduling plan in the worst-case scenario. However, since AC-DC mutual conversions in AC/DC hybrid microgrid are entirely completed through the BC connecting AC bus and DC bus. The operation cost and conversion efficiency of BC have significant impact on the energy management of AC/DC hybrid microgrid. Moreover, the conversion efficiency of BC

is always changing. The above-mentioned factors together constitute the multiple uncertainties of AC/DC hybrid microgrid. Nevertheless, in previous researches, the multiple uncertainties are partially ignored. For instance, the conversion efficiency of BC is often treated as a fixed value or even neglected [29], [31]–[33]. Thus BC schedules will not match the actual BC operation states. In some researches like the reference [10], [20], [30], [34], the scheduling scheme of AC/DC hybrid microgrid is developed by one-time offline energy management model based on day-ahead forecast. As a result, the schedules are may quite different from the actual operation, and even completely deviate in some extreme scenarios.

Given no existing works have addressed the abovementioned problems in one research before, a comprehensive research on the noted issues is indispensable for the economic and robust operation of AC/DC hybrid microgrid. To this end, a temporally coordinated energy management strategy for AC/DC hybrid microgrid is proposed in this paper. The major contributions of this work are presented as follows.

- 1) A novel dynamic conversion efficiency(DCE) model of BC is developed based on the operation and loss characteristics of BC. The model can more accurately reflect the actual BC operation state and effectively reduce the operation cost of the AC/DC hybrid microgrid, especially for the weak light condition day.
- 2) A temporally coordinated energy management strategy for AC/DC hybrid microgrid integrated with DCE model is proposed. The RESs outputs, operation characteristics of microgrid components and time-of-use electricity price are comprehensively considered in the day-ahead economic energy management stage to minimize the daily operation cost. In the intraday rolling energy management stage, day-ahead schedules of controllable units are adjusted based on intraday ultra-short-term forecast data to suppress the intraday power fluctuations induced by day-ahead forecast errors.

The remainder of this paper is organized as follows. Section II describes the structure of AC/DC hybrid microgrid. Section III introduces the DCE model of BC. Section IV illustrates the operation cost models of microgrid components. Section V presents the temporally coordinated energy management strategy for AC/DC hybrid microgrid. Case studies are conducted in Section VI. The conclusions are drawn in Section VII.

II. STRUCTURE OF AC/DC HYBRID MICROGRID

The structure of AC/DC hybrid microgrid studied in this paper is shown in Fig.1. AC bus carries wind turbine (WT) and AC loads, and it's connected to main grid. Fuel cell, photovoltaic (PV) panels, lithium-ion battery (LB) and DC loads are connected to DC bus. The LB in the DC region can achieve the peak clipping/valley filling effect for the entire microgrid. AC bus and DC bus are interconnected through a BC for power exchange between two regions. In working

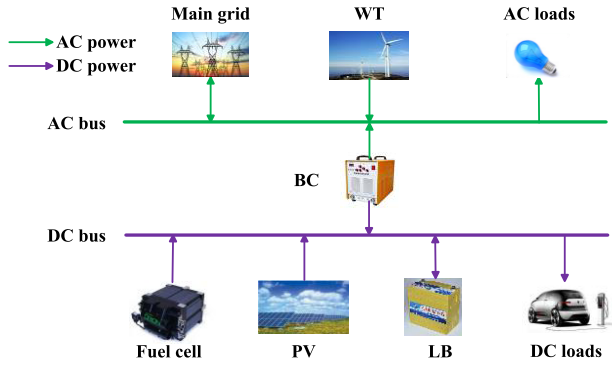


FIGURE 1. Structure of the AC/DC hybrid microgrid.

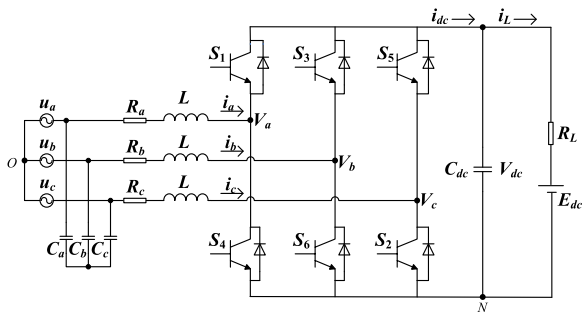


FIGURE 2. Topology of BC.

condition, the AC loads and the DC loads are first powered by the DGs in the corresponding region. When the power imbalance occurs in AC region or DC region, the power can be complemented through the BC.

Obviously, the AC/DC hybrid microgrid separates AC region from DC region by BC to replace numerous AC/DC conversions in traditional AC microgrid. However, since the BC occupies the main body of energy conversions in the AC/DC hybrid microgrid, the conversion efficiency and operation cost of BC have much more significant impact on the energy management than in traditional AC microgrid. However, the conversion efficiency of BC is always changing. In view of that, accurately modeling the conversion efficiency of BC is indispensable to the energy management of the AC/DC hybrid microgrid.

III. DYNAMIC CONVERSION EFFICIENCY MODEL OF BC

This section aims to develop accurate conversion efficiency model of BC. The topology of bidirectional AC/DC power converter is shown in Fig.2.

In the figure, S₁-S₆ are IGBT modules. Relevant studies indicate that converter loss mainly includes IGBT module loss and inductance loss. The loss of the IGBT module is the sum of the conduction loss and the switching loss of IGBTs and diodes [35], [36]. The conduction loss of IGBT is defined as below.

$$P_T = \frac{1}{2\pi} \int_0^\pi u_{CE} i_C D dt + \frac{1}{2\pi} \int_0^\pi u_F i_F (1 - D) dt \quad (1)$$

where u_{CE} and i_C are terminal voltage and current of IGBT, u_F and i_F are terminal voltage and current of diode, D is duty cycle.

Due to i_C is equal to i_F , P_T can be represented by a linear function as

$$P_T = (R_{CE} + R_F) I_C^2 + (U_{CEO} + U_{FO}) I_C \quad (2)$$

where I_C is on-state current, R_{CE} and R_F are on-state equivalent resistance of IGBT and diode, U_{CEO} and U_{FO} are threshold voltage of IGBT and diode.

The switching loss of IGBT module is mainly composed of switching loss of IGBT P_{SI} and reverse recovery loss of diode P_{SD} . According to the product manual:

$$P_{SI} = P_{Son} + P_{Soff} = (a_1 I_C^2 + a_2 I_C + a_3) U_{CE} \quad (3)$$

$$P_{SD} = (a_4 I_C^2 + a_5 I_C + a_6) U_{CE} \quad (4)$$

where U_{CE} is the collector-to-emitter voltage of IGBT, it can be regarded as a constant value in steady state. P_{Son} and P_{Soff} refer to turn-on loss and turn-off loss of IGBT, $a_i (i = 1, 2, \dots, 9)$ refer to the parameters related to the operation.

The inductance loss of converter is mainly copper loss. It is proportional to the square of I_C . Considering (2)-(4), converter loss P_L can be described as

$$P_L = P_T + P_{SI} + P_{SD} + I_C^2 R_L = a_7 I_C^2 + a_8 I_C + a_9 \quad (5)$$

Since U_{CE} is constant under operating condition, I_C is proportional to the converter transmission power P . Thus (5) can be changed to (6).

$$P_L = b_1 P^2 + b_2 P + b_3 \quad (6)$$

where $b_i (i = 1, 2, 3)$ are the parameters related to the operation. Therefore, the conversion efficiency of BC η_{BC} can be drawn as below.

$$\eta_{BC} = (P - P_L)/P = -b_1 P + 1 - b_2 - b_3/P \quad (7)$$

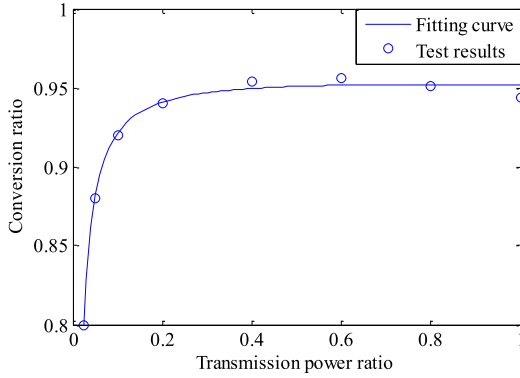
Defining the transmission power ratio P_R as the ratio of the transmission power P to the converter rated power P_N , and then combining the coefficients, η_{BC} can be derived as

$$\eta_{BC} = k_1 P_R + k_2 + k_3/P_R \quad (8)$$

where $k_i (i = 1, 2, 3)$ are the parameters related to the operation, they can be obtained through experimental test.

In this paper, we focus on an existing AC/DC hybrid microgrid in North China. Rated power of BC in this microgrid is 50kW. Fig. 3 shows the test results of the BC and the corresponding conversion efficiency curve fitted by (8). It can be seen that the developed model is accurate.

Since transmission power is positively correlated with transmission power ratio, the BC conversion efficiency is a function of its transmission power according to (8). Conversion efficiency varies in a relatively large range at different transmission power. This means that the conversion efficiency of BC is not just a constant coefficient as in the traditional research, but will participate in the microgrid scheduling. In the optimization problem of microgrid energy


FIGURE 3. Conversion efficiency curve of BC.

management, the conversion efficiency is actually defined as a decision variable. It plays the same role as other decision variables. It is determined by the transmission power, which is closely related to the dynamic relationship of power balance between AC region and DC region. Therefore, compared with the traditional model, the dynamic conversion efficiency denoted by (8) is particularly significant for the energy management of AC/DC hybrid microgrid.

The cost of BC is mainly divided into two parts: operation and maintenance cost and power loss cost. Therefore, the cost can be expressed as:

$$\begin{cases} C_{BC,t} = C_{BCOM,t} + C_{BCL,t} \\ C_{BCOM,t} = K_{BCOM} (P_{BC,t}^{AC} + P_{BC,t}^{DC}) \Delta t \\ C_{BCL,t} = C_{P,t} (1 - \eta_{BC,t}) (P_{BC,t}^{AC} + P_{BC,t}^{DC}) \Delta t \end{cases} \quad (9)$$

where $C_{BCOM,t}$ and $C_{BCL,t}$ are operation and maintenance cost and power loss cost of BC at time interval t , $P_{BC,t}^{AC}$ or $P_{BC,t}^{DC}$ is power flow from AC or DC to the BC at time interval t , K_{BCOM} is the operation and maintenance cost coefficient of BC, $C_{P,t}$ is electricity price of main grid at time interval t .

The BC operation should satisfy the following constraints:

$$\begin{cases} 0 \leq P_{BC,t}^{AC} \leq I_{BC,t}^{AC} P_{BCmax} \\ 0 \leq P_{BC,t}^{DC} \leq I_{BC,t}^{DC} P_{BCmax} \\ I_{BC,t}^{AC} + I_{BC,t}^{DC} \leq 1 \\ P_{BC,t} = P_{BC,t}^{DC} - P_{BC,t}^{AC} \end{cases} \quad (10)$$

where P_{BCmax} is the maximum transmission power of the BC, $P_{BC,t}$ is the power injected to the converter at time interval t , assuming a positive value for the DC side injection, a negative value for the AC side injection. $I_{BC,t}^{AC}$ and $I_{BC,t}^{DC}$ are the power flow direction indicator of the BC. They are binary variables, " $I_{BC,t}^{AC} = 1$ " represents that the transmission power from the AC side to the DC side, whereas " $I_{BC,t}^{DC} = 1$ " is the opposite.

IV. COST MODELS OF AC/DC HYBRID MICROGRID

This section presents cost models for fuel cell, LB and power exchange with main grid.

A. COST MODEL OF FUEL CELL

The cost of fuel cell at time interval t $C_{FC,t}$ can be given as below.

$$\begin{cases} C_{FC,t} = C_{FCO,t} + C_{FCM,t} \\ C_{FCO,t} = \frac{C_F P_{FC,t}}{Q_{LHV} \eta_{FC}} \Delta t \\ C_{FCM,t} = K_{FCM} P_{FC,t} \Delta t \end{cases} \quad (11)$$

where $C_{FCO,t}$, $C_{FCM,t}$ and $P_{FC,t}$ represent operation cost, maintenance cost and power of fuel cell at time interval t , respectively; C_F is gas price, Q_{LHV} is lower heating value of gas, Δt is length of time interval; η_{FC} and K_{FCM} are efficiency and maintenance cost coefficient of fuel cell.

The output power of the fuel cell is constrained by:

$$P_{FCmin} \leq P_{FC,t} \leq P_{FCmax} \quad (12)$$

where P_{FCmin} and P_{FCmax} are the minimum and maximum output power of the fuel cell.

B. COST MODEL OF LB

According to the discharge depth model based on rain-flow counting method [37] and the loss model based on throughput estimation method [38], operation cost of LB at time interval t $C_{liO,t}$ can be described as below.

$$\begin{aligned} C_{liO,t} &= \frac{C_{in} (P_{ch,t} + P_{dis,t})}{2N_{rl,t} E_{rc}} \Delta t \\ N_{rl,t} &= -3278D_{od,t}^4 - 5D_{od,t}^3 \\ &\quad + 12823D_{od,t}^2 - 14122D_{od,t} + 5112 \end{aligned} \quad (13) \quad (14)$$

where $P_{ch,t}$ and $P_{dis,t}$ are charge power and discharge power of LB, C_{in} is the initial investment cost, $N_{rl,t}$ and E_{rc} are cycle life and rated power of LB, $D_{od,t}$ is discharge depth of LB.

The cost of LB at time interval t $C_{li,t}$ is expressed as follows.

$$C_{li,t} = C_{liO,t} + C_{liM,t} \quad (15)$$

$$C_{liM,t} = K_{liM} (P_{ch,t} + P_{dis,t}) \Delta t \quad (16)$$

where $C_{liM,t}$ represents maintenance cost of LB at time interval t , K_{liM} is the maintenance cost coefficient of LB.

The operation of LB should meet the following constraints:

$$\begin{cases} 0 \leq P_{ch,t} \leq I_{ch,t} P_{limax} \\ 0 \leq P_{dis,t} \leq I_{dis,t} P_{limax} \\ I_{ch,t} + I_{dis,t} \leq 1 \\ P_{li,t} = P_{dis,t} - P_{ch,t} \end{cases} \quad (17)$$

$$\begin{cases} SOC_t = \frac{E_{r,t}}{E_{rc}} \\ SOC_{min} \leq SOC_t \leq SOC_{max} \\ E_{r,t} = E_{r,t-1} + \eta_{li} P_{ch,t} - \frac{P_{dis,t}}{\eta_{li}} \\ E_{r,0} = E_{r,T} \end{cases} \quad (18) \quad (19)$$

where P_{limax} is the maximum charge/discharge power of the LB, $P_{li,t}$ is the power of the LB at time interval t , assuming

a positive value for the discharge mode, a negative value for the charge mode. $I_{ch,t} / I_{dis,t}$ represents the charge/ discharge mode indicator of the LB (“1” represents that the LB is in charge/discharge mode, “0” otherwise). (18) shows the capacity constraints, where SOC_t is the state of charge (SOC) of the LB at time interval t , SOC_{min} and SOC_{max} are the minimum and maximum SOC of the LB, $E_{r,t}$ is the remaining capacity of the LB at time interval t , η_{li} is the efficiency of the LB. (19) limits the initial and final remaining capacity of the LB in the energy management cycle, where $E_{r,0}$ and $E_{r,T}$ are initial and final remaining capacity of the LB. In order to ensure the long-term implement of the energy management, the remaining capacity of the LB should be periodic.

C. COST MODEL OF POWER EXCHANGE WITH MAIN GRID

The cost of power exchange with main grid at time interval t $C_{grid,t}$ is defined as below.

$$C_{grid,t} = (C_{P,t}P_{Pgrid,t} - C_{S,t}P_{Sgrid,t}) \Delta t \quad (20)$$

where $C_{P,t}$ and $C_{S,t}$ are power purchase price from main grid and sale price to main grid at time interval t , $P_{Pgrid,t}$ is power flow from main grid to microgrid at time interval t , whereas $P_{Sgrid,t}$ is the opposite.

The power exchange should satisfy the following constraints:

$$\begin{cases} 0 \leq P_{Pgrid,t} \leq I_{Pgrid,t}P_{gridmax} \\ 0 \leq P_{Sgrid,t} \leq I_{Sgrid,t}P_{gridmax} \\ I_{Pgrid,t} + I_{Sgrid,t} \leq 1 \\ P_{grid,t} = P_{Pgrid,t} - P_{Sgrid,t} \end{cases} \quad (21)$$

where $P_{gridmax}$ is the maximum exchanged power of the tie-line, $P_{grid,t}$ is the exchanged power of the tie-line at time interval t , assuming a positive value for purchasing electricity from main grid, a negative value for selling electricity to main grid. $I_{Pgrid,t}$ and $I_{Sgrid,t}$ are binary variables that determine the states of the microgrid purchasing electricity from or selling electricity to the main grid, respectively.

V. TEMPORALLY COORDINATED ENERGY MANAGEMENT STRATEGY FOR AC/DC HYBRID MICROGRID

Compared with the traditional AC microgrid, the source-load uncertainties both exist in the AC and DC regions, which brings great challenges to the energy management. Many forecasting methods have been developed in the literature [39], [40], the results show that the short-term forecast tends to be more accurate than the long-term one, hence the impact of uncertainties can be better mitigated in the short-term operation timescale. To this end, a temporally coordinated energy management strategy for AC/DC hybrid microgrid is proposed in this paper. The strategy includes two stages: day-ahead economic energy management and intraday rolling energy management. The energy management framework is shown in Fig.4.

In the day-ahead economic energy management stage, a day-ahead hourly schedule is determined to minimize the

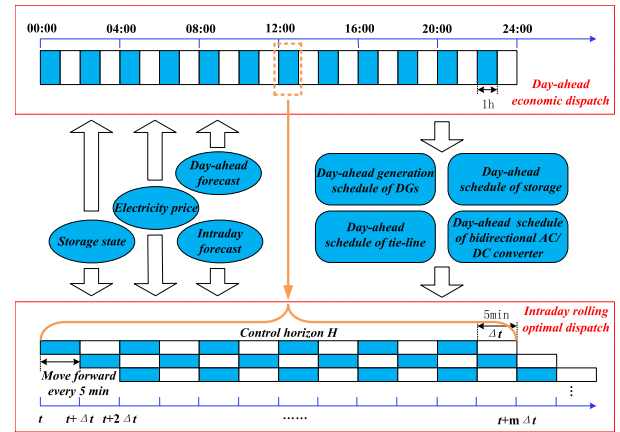


FIGURE 4. Temporally coordinated energy management framework of AC/DC hybrid microgrid.

daily operation cost based on the forecast data of PV, WT and loads. The RESs outputs, operation characteristics of microgrid components and time-of-use electricity price are comprehensively considered in the model.

In the intraday rolling energy management stage, the dynamic fluctuations of PV, WT and loads should be accommodated in the operation of microgrid. Therefore, a rolling horizon optimization strategy is employed to adjust the day-ahead scheduling based on the intraday ultra-short-term forecast data. Moreover, to ensure the effectiveness of the day-ahead schedules, the strategy also track the day-ahead schedules of BC and the SOC of LB as close as possible. The time scale of the stage is 5 min and the control horizon is 1 h (covers 12 intervals). At each time step, schedules for each interval in the control horizon are developed. But only the first 5min-interval schedule is executed, while the rest of schedules are regarded as references. Then, at the next time step, the control horizon moves forward by 5 min as illustrated in Fig. 4. The model inputs will be updated and the above process will be repeated. The control horizon moves forward 288 times in one day.

A. DAY-AHEAD ECONOMIC ENERGY MANAGEMENT

The objective of the day-ahead economic energy management is to minimize the operation cost of AC/DC hybrid microgrid. The objective function can be expressed as follows:

$$\min C_{DA} = \sum_{t=1}^T (C_{FC,t} + C_{li,t} + C_{BC,t} + C_{grid,t}) \quad (22)$$

where C_{DA} is day-ahead total cost of the AC/DC hybrid microgrid, T is the total number of dispatch time periods. The formulations of $C_{BC,t}$, $C_{FC,t}$, $C_{li,t}$ and $C_{grid,t}$ are given in (9), (11), (15) and (20), respectively.

Considering the operation mode of AC/DC hybrid microgrid and the operation characteristics of DGs, ESs and converters, the constraints that need to be met are as follows.

(1) Operation balance constraints of AC/DC hybrid microgrid:

The operation balance constraints of the AC-DC hybrid microgrid include the overall operational balance constraints and the respective balance constraints of the AC and DC regions.

$$P_{PV,t} + P_{WT,t} + P_{FC,t} + P_{Pgrid,t} - P_{Sgrid,t} + P_{dis,t} - P_{ch,t} = P_{Lac,t} + P_{Ldc,t} + (1 - \eta_{BC,t}) (P_{BC,t}^{AC} + P_{BC,t}^{DC}) \quad (23)$$

$$P_{WT,t} + P_{Pgrid,t} - P_{Sgrid,t} = P_{Lac,t} + P_{BC,t}^{AC} - \eta_{BC,t} P_{BC,t}^{DC} \quad (24)$$

$$P_{PV,t} + P_{FC,t} + P_{dis,t} - P_{ch,t} = P_{Ldc,t} + P_{BC,t}^{DC} - \eta_{BC,t} P_{BC,t}^{AC} \quad (25)$$

where $P_{PV,t}$ and $P_{WT,t}$ are power of PV and WT at time interval t , $P_{Lac,t}$ and $P_{Ldc,t}$ are AC loads and DC loads at time interval t . Particularly, $\eta_{BC,t}$ employs the DCE model of BC, which is defined in (8).

(2) Components constraints:

Constraints of BC, fuel cell, LB and tie-line are presented in (10),(12),(17-19) and (21), respectively.

B. INTRADAY ROLLING ENERGY MANAGEMENT

As time scale shortens, the forecast accuracy improves. Therefore, the intraday rolling energy management of AC/DC hybrid microgrid based on intraday ultra-short-term forecast data can effectively reduce the negative impacts of day-ahead forecast errors.

The objective of intraday rolling energy management is to minimize the variation resulted from day-ahead forecast errors while tracking the day-ahead scheduling of the BC and the SOC of LB as close as possible. The model consists of two parts: rolling prediction model and optimization problem modeling.

1) ROLLING PREDICTION MODEL

The rolling prediction model is developed to predict the control variables in the control horizon, that is, to realize the power prediction of DGs, ESs and BC in the AC/DC hybrid microgrid. The model can be expressed as follows.

$$\begin{cases} P_{FC}(t + k\Delta t|t) = P_{FC,t} + \sum_{i=1}^k \Delta P_{FC}(t + i\Delta t|t) \\ P_{li}(t + k\Delta t|t) = P_{li,t} + \sum_{i=1}^k \Delta P_{li}(t + i\Delta t|t) \\ k = 1, 2, \dots, m \\ P_{BC}(t + k\Delta t|t) \\ = P_{BC,t} + \sum_{i=1}^k \Delta P_{PV}(t + i\Delta t|t) \\ + \sum_{i=1}^k \Delta P_{FC}(t + i\Delta t|t) + \sum_{i=1}^k \Delta P_{li}(t + i\Delta t|t) \end{cases} \quad (26)$$

$$-\sum_{i=1}^k \Delta P_{Ldc}(t + i\Delta t|t) \quad k = 1, 2, \dots, m \quad (27)$$

$$\begin{aligned} SOC(t + k\Delta t|t) \\ = SOC[t + (k - 1)\Delta t|t] - \frac{P_{li}(t + k\Delta t|t)}{\lambda E_{rc}} \\ k = 1, 2, \dots, m \end{aligned} \quad (28)$$

(26) provides the rolling prediction model of the fuel cell and the LB. Rolling prediction models of output variables are further derived in (27), (28) based on power balance of the AC/DC hybrid microgrid and SOC iterative formula of LB, where m represents the number of dispatch time periods in the control horizon. $\mathbf{x}_t(t + k\Delta t|t)$ is the state of \mathbf{x}_t at the time $t + k\Delta t$ predicted at time t (\mathbf{x}_t can be P_{FC} , P_{li} , P_{BC} or SOC). $\mathbf{u}_t(t + k\Delta t|t)$ or $\mathbf{r}_t(t + k\Delta t|t)$ denotes the power variation of the time $t + i\Delta t$ previous period predicted at time t (\mathbf{u}_t can be ΔP_{FC} or ΔP_{li} , whereas \mathbf{r}_t can be ΔP_{PV} , ΔP_{WT} , ΔP_{Lac} or ΔP_{Ldc}). λ refers to the number of dispatch time periods per hour.

2) OPTIMIZATION PROBLEM MODELING

To minimize the power variations resulted from day-ahead forecast errors while tracking the day-ahead scheduling of the BC and the SOC of LB as close as possible, objective function of the intraday rolling energy management model are formulated as follows.

$$\min f = \|\mathbf{Y} - \mathbf{Y}_{ref}\|_{\mathbf{G}}^2 + \|\mathbf{U}\|_{\mathbf{H}}^2 \quad (29)$$

$$\begin{aligned} \mathbf{Y} = [P_{BC}(t + \Delta t|t), SOC(t + \Delta t|t), \dots, \\ P_{BC}(t + m\Delta t|t), SOC(t + m\Delta t|t)] \quad (30) \\ \mathbf{Y}_{ref} = [P_{BC,t+\Delta t}^{ref}, SOC_{t+\Delta t}^{ref}, \dots, P_{BC,t+m\Delta t}^{ref}, SOC_{t+m\Delta t}^{ref}] \quad (31) \end{aligned}$$

$$\begin{aligned} \mathbf{U} = [\Delta P_{FC}(t + \Delta t|t), \Delta P_{li}(t + \Delta t|t), \dots, \\ \Delta P_{FC}(t + m\Delta t|t), \Delta P_{li}(t + m\Delta t|t)] \quad (32) \end{aligned}$$

$$\text{s.t. } P_{FCmin} \leq P_{FC}(t + k\Delta t|t) \leq P_{FCmax} \quad (33)$$

$$\Delta P_{FCmin} \leq \Delta P_{FC}(t + k\Delta t|t) \leq \Delta P_{FCmax} \quad (34)$$

$$P_{limin} \leq P_{li}(t + k\Delta t|t) \leq P_{limax} \quad (35)$$

$$\Delta P_{limin} \leq \Delta P_{li}(t + k\Delta t|t) \leq \Delta P_{limax} \quad (36)$$

$$P_{BCmin} \leq P_{BC}(t + k\Delta t|t) \leq P_{BCmax} \quad (37)$$

$$P_{gridmin} \leq P_{grid}(t + k\Delta t|t) \leq P_{gridmax} \quad (38)$$

$$SOC_{min} \leq SOC(t + k\Delta t|t) \leq SOC_{max} \quad (39)$$

where \mathbf{Y} , \mathbf{Y}_{ref} and \mathbf{U} are output vector, objective vector and control vector, respectively. In the objective vector \mathbf{Y}_{ref} , the day-ahead schedules of transmission power of BC and the SOC of LB are selected as reference objectives. \mathbf{G} and \mathbf{H} are the difference weight vector and the control weight vector, they are both diagonal matrixes, ΔP_{FCmin} and ΔP_{FCmax} are the minimum and maximum output power variations of the fuel cell, whereas ΔP_{limin} and ΔP_{limax} are the minimum and maximum output power variations of the LB. In above constraints, $k = 1, 2, \dots, m$. Additionally, the model is also constrained by operation balance denoted by (23).

TABLE 1. Operation parameters of AC/DC hybrid microgrid.

Fuel cell	C_F	1.81 $\text{\$/m}^3$	Q_{LHV}	9.7kWh/ m^3
	η_{FC}	40%	K_{FCM}	0.1 $\text{\$/ kWh}$
	P_{FCmin}	0	P_{FCmax}	5kW
	ΔP_{FCmin}	-5kW	ΔP_{FCmax}	5kW
LB	K_{liM}	0.0832 $\text{\$/kWh}$	η_{li}	0.9
	SOC_{min}	0.2	SOC_{max}	0.9
	P_{limin}	-25kW	P_{limax}	25kW
	ΔP_{limin}	-25kW	ΔP_{limax}	25kW
	E_{rc}	26 kWh		
BC	K_{BCOM}	0.02 $\text{\$/kWh}$	P_{BCmin}	-50kW
	P_{BCmax}	50kW	k_1	-0.0067
	k_2	-0.004	k_3	0.9623
Tie-line	$P_{gridmax}$	-100kW	$P_{gridmin}$	100kW
PV	Rated power			30kW
WT	Rated power			5kW

The optimal sequence can be acquired by solving the above problem, and the first element of the sequence is applied. By repeating the process at the following time steps, the intraday rolling energy management will be completed.

Additionally, the paper focuses on the economy problem of AC/DC hybrid microgrid under multiple uncertainties. The normal operation of microgrid is the precondition of this paper. Generally speaking, under the grid connected operation mode, the shutdown of a certain equipment will not affect the normal operation of the microgrid. If the main grid is cut off, the microgrid will automatically switch to island operation mode. Many literatures such as microgrid reliability, control and reconstruction have investigated corresponding approaches to deal with the above-mentioned situations. But these situations will not be further discussed since these are out of the scope of this paper.

VI. CASE STUDIES

Based on an existing AC/DC hybrid microgrid in North China, this section studies the effectiveness of the temporally coordinated energy management strategy for AC/DC hybrid microgrid. The structure of the microgrid is shown in Fig.1. The operation parameters of AC/DC hybrid microgrid are listed in Table 1.

Real data sets from the AC/DC hybrid microgrid in North China on a typical sunny day (July 25, 2018) are employed for the case studies. Day-ahead and intraday ultra-short-term forecast data for PV, WT and AC/DC loads are shown in Figs. 5-7, respectively. Their errors between the day-ahead forecast and the intraday ultra-short-term forecast are 13.6%, 16.5%, 11.3% and 10.2%, respectively. The reason why the data sets are chosen is that they can statistically best represent

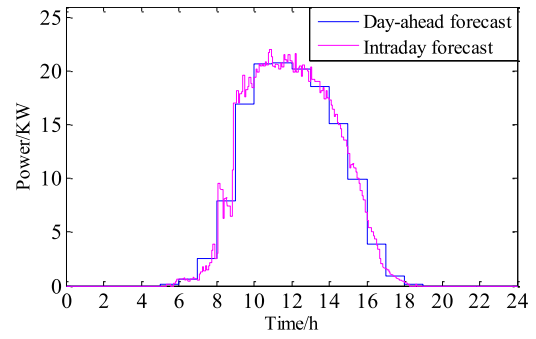


FIGURE 5. Forecast power of PV.

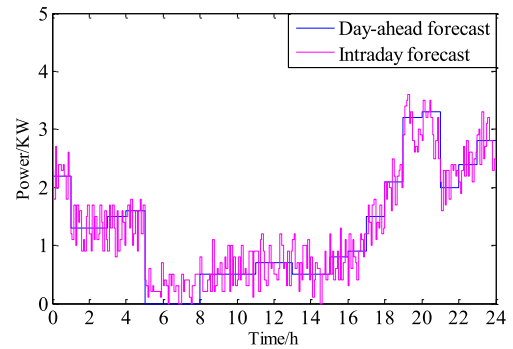


FIGURE 6. Forecast power of WT.

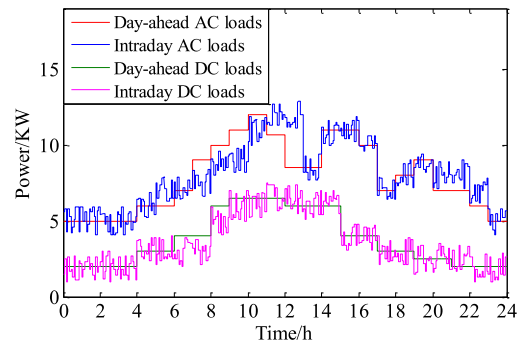


FIGURE 7. Forecast power of AC/DC loads.

the general level of our microgrid energy management system forecast module.

The time-of-use electricity price of main grid is shown in Fig.8. All the simulations are implemented using particle swarm optimization (PSO) algorithm in MATLAB on a 64-bit PC with Intel(R) Core(TM) i7-8700 CPU @3.2 GHz and 16 GB memory.

A. DAY-AHEAD ECONOMIC ENERGY MANAGEMENT RESULTS ANALYSIS

According to the day-ahead economic energy management model developed in this paper, the energy management results of the AC/DC hybrid microgrid are presented in Fig.9.

The analyses of the day-ahead economic energy management results are as follows:

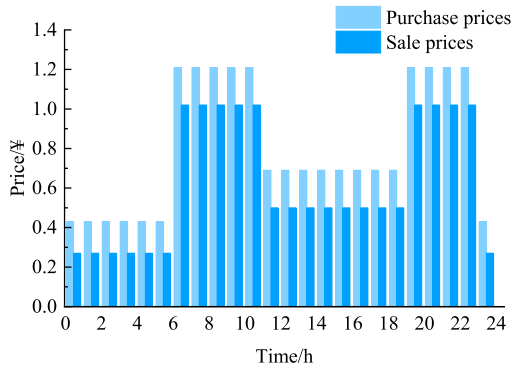


FIGURE 8. Time-of-use electricity prices of main grid.

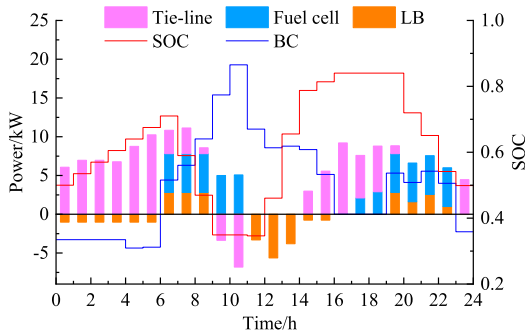


FIGURE 9. Day-ahead energy management results of the AC/DC hybrid microgrid.

1) During the valley periods (23:00-6:00), both AC and DC loads are low, and the PV power in DC region is close to 0. Whereas the WT power in AC region is large, and the microgrid purchases electricity from the main grid. Apart from meeting the AC loads, power flows into the DC side through BC, and the transmission power of the BC is negative. During the off-valley periods, since the PV power in DC region is large and the LB is largely discharged, the DC side power flows to the AC side, and the transmission power of the BC is mainly positive. During the period 16:00-19:00, the transmission power of the BC is 0. That's because the comprehensive cost for power exchanging between the AC and DC regions is higher than purchasing electricity from the main grid in the period.

2) At night, the WT power is sufficient and the purchase price is in the valley price. The LB SOC reaches a high value after charging at night. In the morning, the WT power is reduced and the PV power is still insufficient. As the load demand increases, the LB switches to the discharge mode and the SOC gradually reaches a low value. Thus the microgrid can sell electricity to the main grid while meeting the load demand. At noon, the PV power reaches the peak value of the day, the LB switches to the charge mode again. Then the SOC returns to a high value. During the peak period (19:00-23:00), PV power stops and LB discharges. The LB SOC eventually returns to the initial value of the energy management start to ensure the periodicity of energy management. In summary,

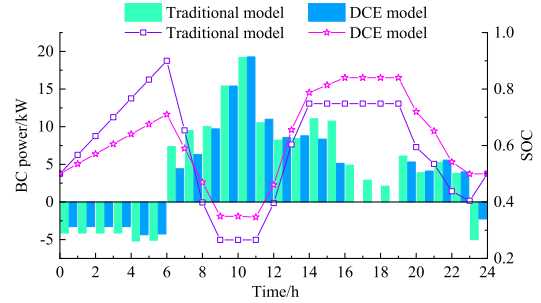


FIGURE 10. The BC transmission power and the LB SOC based on different conversion efficiency models.

TABLE 2. Comparison of different conversion efficiency models.

Conversion efficiency model	Operation cost(¥)	Computation time(s)
Traditional model	87.74	0.87
DCE model	85.23	46.35

the LB not only effectively plays the role of “peak clipping/valley filling”, but also can benefit for microgrid from the peak-to-valley electricity price difference.

B. COMPARISON OF DIFFERENT BC CONVERSION EFFICIENCY MODELS

In this paper, the DCE model of BC is presented based on the operation and loss characteristics of BC. To evaluate rationality and effectiveness of the model, the traditional model is adopted for comparison in this section. In the traditional model, the BC conversion efficiency is a constant and its value is set to 0.95 in this simulation. In the day-ahead economic energy management, the above two models are adopted respectively.

Fig.10 shows the BC transmission power and the LB SOC based on different conversion efficiency models. In the figure, the histogram is the BC transmission power and the line chart is the LB SOC. Table 2 lists the operation costs of day-ahead schedules and the corresponding computation time based on different conversion efficiency models. The operation cost here refers to the actual day-ahead operation cost. To fairly assess the performance of the two models, the conversion efficiency of the traditional model also adopts the actual conversion efficiency. The day-ahead schedules of the controllable units are unchanged, and the tie-line power is obtained according to the power balance. Then, the actual day-ahead operation cost is calculated accordingly. In this way, the operation cost is accurate. It makes the day-ahead operation costs based on the two conversion efficiency models follow the unified standard. Additionally, the actual conversion efficiencies of traditional model are calculated based on the day-ahead BC schedules using the conversion efficiency curve shown in Fig. 3.

Obviously, DCE model has longer computation time, but the lower operation cost. Although the traditional model

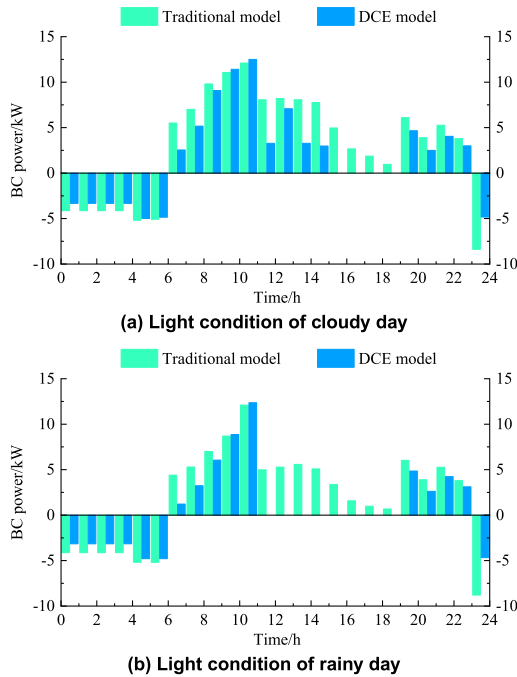


FIGURE 11. The BC transmission power under different light conditions.

has a shorter computation time, it cannot accurately reflect the actual operation state, which leads to higher operation cost. For instance, during the period 16:00-19:00 in Fig.10, the required exchanged power between the AC and DC regions decreases significantly. Thus the conversion efficiency greatly declines according to the BC transmission characteristics. As a result, the power exchange cost between the AC and DC regions will be higher than purchasing electricity from the main grid. Therefore, the BC transmission power based on the DCE model drops to 0. However, since the BC conversion efficiency is a constant in the traditional model, the power exchange cost consistently keeps lower than purchasing electricity from the main grid. Therefore, there is always power exchange between the AC and DC regions. But this is obviously inconsistent with the actual operation state, which will eventually lead to higher operation cost. Moreover, as shown in Fig.10, when DCE model is adopted, the range of LB SOC is smaller than that of traditional model. This is beneficial to prolong the cycle life of LB.

The above simulation implements on a typical sunny day. Fig.11 respectively shows the BC transmission power under light condition of cloudy day and rainy day based on different conversion efficiency models. For comparison, the WT output power, load profiles and electricity price are the same as the above simulation which are shown in Figs.6-7, respectively. Table 3 shows the operation cost deviations between the two conversion efficiency models under different light conditions, as well as the sum of their transmission power absolute deviations.

As shown in Fig.11 and Table 3, under light condition of cloudy day and rainy day, transmission power absolute

TABLE 3. Comparison under different light conditions.

Light conditions	$\Delta C_{DA}(\text{¥})$	$\sum \Delta P_{BC} (\text{KW})$
Sunny	2.51	35.2
Cloudy	3.62	44.3
Rainy	4.16	47.1

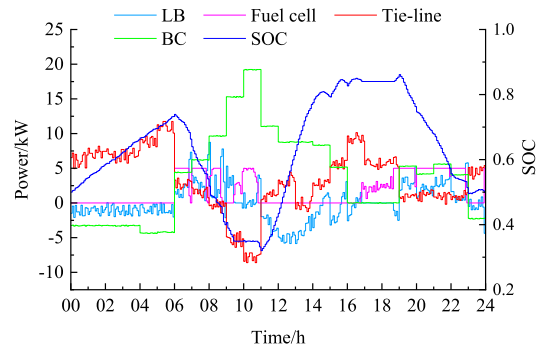


FIGURE 12. Intraday energy management results of AC/DC hybrid microgrid.

deviations between the two conversion efficiency models are higher than that of sunny day. Accordingly, they have more operation cost deviations. In other words, under light condition of cloudy day and rainy day, more operation costs are saved than sunny day based on DCE model. This is because PV output power under light condition of cloudy day and rainy day are much less than sunny day, which results in less required exchanged power between the AC and DC regions. Due to the wide range of transmission efficiency corresponding to the relatively lower transmission power in the DCE model, the economic performances of the model are better than sunny day. For instance, in Fig.11(b), because of the less required exchanged power there is no transmission power during the period 12:00-19:00 based on the DCE model. That is a sufficient reflection for the above statement.

In summary, the proposed DCE model of BC can more accurately reflect the BC operation state and effectively reduce the operation cost of the AC/DC hybrid microgrid, especially for the weak light condition day. Moreover, the model is beneficial to prolong the cycle life of LB. Furthermore, with the increase of microgrid capacity and user loads, the economic benefits of the DCE model will be further amplified. In addition, although the model needs longer computation time, it won't be the computational burden for online application because of the high-performance computer and more advanced algorithms.

C. INTRADAY ROLLING ENERGY MANAGEMENT RESULTS ANALYSIS

According to the intraday rolling energy management model presented in this paper, the energy management results of the AC/DC hybrid microgrid are shown in Fig.12.

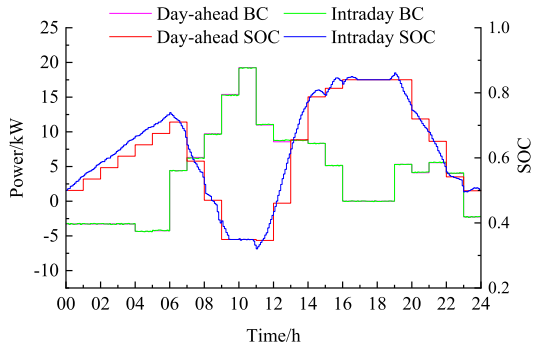


FIGURE 13. Tracking effects of the BC transmission power and LB SOC.

Certain adjustments are implemented to the day-ahead schedules based on intraday ultra-short-term forecast data. The intraday additional cost is 20.19¥, and the total operation cost is 105.42¥. However, without the intraday rolling energy management, the intraday power fluctuations will be merely suppressed by main grid through the tie-line. In that case, the intraday additional cost will reach 28.56¥, 34.1% higher than the proposed strategy. Therefore, the intraday rolling energy management of AC/DC hybrid microgrid can effectively reduce the negative impacts of day-ahead forecast errors to achieve the excellent overall economic performance.

Fig. 13 illustrates the tracking effects of the BC transmission power and LB SOC. It can be seen that the intraday BC transmission power and LB SOC follow the day-ahead schedules well. Therefore, intraday rolling energy management of AC/DC hybrid microgrid not only reduces the negative impacts of day-ahead forecast errors, but also ensures the effectiveness of the day-ahead schedules. Moreover, the accurate tracking of BC transmission power also effectively guarantees the stable and robust operation of the AC/DC hybrid microgrid in real time.

D. COMPARISON ANALYSIS OF DIFFERENT OPTIMIZATION STRATEGIES

To evaluate the performance of the proposed strategy, the test data with different levels of forecast uncertainty are generated according to the following equations.

$$P_{j,t}^{ID} = P_{j,t}^{DA} [1 + \xi_j\% \cdot (R_{j,t} - 0.5)] \quad (40)$$

$$f(R_{j,t}) = R_{j,t}^{\alpha-1} \cdot (1 - R_{j,t})^{\beta-1} \cdot N \quad (41)$$

$$f(R_{j,t}) = \frac{1}{\sigma\sqrt{2\pi}} \exp\left(-\frac{(R_{j,t} - \mu)^2}{2\sigma^2}\right) \quad (42)$$

where $P_{j,t}^{ID}$ and $P_{j,t}^{DA}$ are intraday ultra-short-term forecast value and day-ahead forecast value, j can be PVs, WTs, AC and DC loads, $\xi_j\%$ is the uncertainty threshold percentage of day-ahead forecast, $R_{j,t}$ is a random number following a certain distribution.

For RES units like WTs and PVs, their day-ahead forecast errors usually follow the beta distribution which is denoted by (41)[24]. It is defined by two shape parameters: α and β . N

TABLE 4. Uncertainty threshold percentage of day-ahead forecast under different uncertainty levels.

Uncertainty level	Low	Medium	High
PVs	8%	16%	24%
WTs	10%	25%	40%
AC loads	5%	10%	15%
DC loads	5%	10%	15%

represents the normalization factor. Nevertheless, AC and DC loads are mainly determined by human behaviors, the normal distribution denoted by (42) is employed to describe their forecast errors [41]. μ and σ refers to the mean and standard deviation of normal distribution. In this paper, α and β are set to 2.5, μ and σ are set to 0.5 and 0.33, respectively.

According to the uncertainty threshold percentage of day-ahead forecast $\xi_j\%$, the test data is divided into three levels of uncertainty: low, medium and high. Each level has 100 random sets of numbers. Table 4 shows the uncertainty threshold percentage $\xi_j\%$ of PVs, WTs, AC loads and DC loads.

To fully verify the advantage of the proposed strategy, three classical strategies in the literature are compared based on the above generated data.

1) *Case 1: Day-ahead deterministic energy management.* The optimal schedules of the controllable units in microgrid are determined at the day-ahead stage and no uncertainties are considered.

2) *Case 2: Stochastic energy management.* The uncertain information of RESs and loads are described by random variables. The stochastic optimization model is developed by stochastic analysis to acquire the minimum cost scheduling.

3) *Case 3: Robust energy management.* The uncertain information is also described by random variable. But the random variables are confined in a predefined uncertainty set and the optimal scheduling in the worst-case scenario are finally obtained.

4) *Case 4: The proposed temporally coordinated energy management.*

For the 3 groups of test data with different forecast uncertainty levels, the average total operation costs and the growth rates of the operation costs are listed in Table 5.

In Table 5, the average costs of case 1 are the highest under different uncertainty levels. This is because the uncertainties are completely not considered in case 1. Although the uncertainties are both adequately modeled in case 2 and case 3, the average costs of case 3 are higher than case 2 since the robust energy management is more conservative. Due to the two-stage coordinated optimal framework, case 4 has the best economic performance under different uncertainty levels. In terms of the growth rate, case 4 increases the slowest with the increase of uncertainty level. This clearly implies that case 4 shows better robustness under forecast uncertainties. Since the paper’s research object is a grid-connected microgrid. The presented strategy is more inclined to economy performance.

TABLE 5. Results of comparative cases.

Cases	Item	Low-level	Medium-level	High-level
Case 1	Average cost(¥)	108.86	113.78	120.79
	Growth rate	N/A	4.52%	6.16%
Case 2	Average cost(¥)	106.17	110.25	116.77
	Growth rate	N/A	3.84%	5.91%
Case 3	Average cost(¥)	109.43	112.34	117.92
	Growth rate	N/A	2.66%	4.97%
Case 4	Average cost(¥)	101.42	105.31	110.13
	Growth rate	N/A	3.84%	4.58%

Nevertheless, the robustness of the strategy is well guaranteed on the premise of ensuring the economy.

In summary, the above results demonstrate the general superiority of the proposed temporally coordinated energy management strategy in terms of economic performance under forecast uncertainties. Moreover, since the outstanding capability in tracking day-ahead schedules, the stable and robust operation of the AC/DC hybrid microgrid in real time is effectively guaranteed, which is a unique advantage of the proposed strategy.

VII. CONCLUSION

To address multiple uncertainties concerns of AC/DC hybrid microgrid, this paper presents a temporally coordinated energy management strategy integrated with DCE model. The novel DCE model which is developed based on the operation and loss characteristics of BC can accurately reflect the actual BC operation state and reduce the operation cost. The temporally coordinated energy management strategy can effectively deal with the source-load uncertainties.

The simulation results demonstrate that: 1) The proposed DCE model of BC can accurately reflect the BC operation state and effectively reduce the operation cost of the AC/DC hybrid microgrid, especially for the weak light condition day. Meanwhile, the model is also beneficial to prolong the cycle life of LB. 2) The test groups with different uncertainty levels are employed to evaluate the proposed energy management strategy and the classical strategies in the literature. The results manifest the general superiority of the proposed temporally coordinated energy management strategy in terms of economic performance under forecast uncertainties. 3) Since the outstanding capability in tracking day-ahead schedules, the intraday stable and robust operation of the AC/DC hybrid microgrid is well guaranteed on the premise of ensuring the economy.

REFERENCES

[1] D. E. Olivares, A. Mehrizi-Sani, A. H. Etemadi, C. A. Cañizares, R. Iravani, M. Kazerani, A. H. Hajimiragha, O. Gomis-Bellmunt, M. Saadifard, R. Palma-Behnke, G. A. Jiménez-Estévez, and N. D. Hatziargyriou, "Trends in microgrid control," *IEEE Trans. Smart Grid*, vol. 5, no. 4, pp. 1905–1919, Jul. 2014.

[2] C.-S. Karavas, G. Kyriakarakos, K. G. Arvanitis, and G. Papadakis, "A multi-agent decentralized energy management system based on distributed intelligence for the design and control of autonomous polygeneration microgrids," *Energy Convers. Manage.*, vol. 103, pp. 166–179, Oct. 2015.

[3] C. Marnay, G. Venkataramanan, M. Stadler, A. S. Siddiqui, R. Firestone, and B. Chandran, "Optimal technology selection and operation of commercial-building microgrids," *IEEE Trans. Power Syst.*, vol. 23, no. 3, pp. 975–982, Aug. 2008.

[4] Q. Jiang, M. Xue, and G. Geng, "Energy management of microgrid in grid-connected and stand-alone modes," *IEEE Trans. Power Syst.*, vol. 28, no. 3, pp. 3380–3389, Aug. 2013.

[5] C.-S. Karavas, K. Arvanitis, and G. Papadakis, "A game theory approach to multi-agent decentralized energy management of autonomous polygeneration microgrids," *Energies*, vol. 10, no. 11, p. 1756, 2017.

[6] D. Zhang, S. Evangelisti, P. Lettieri, and L. G. Papageorgiou, "Economic and environmental scheduling of smart homes with microgrid: DER operation and electrical tasks," *Energy Convers. Manage.*, vol. 110, pp. 113–124, Feb. 2016.

[7] X. Jin, J. Wu, Y. Mu, M. Wang, X. Xu, and H. Jia, "Hierarchical microgrid energy management in an office building," *Appl. Energy*, vol. 208, pp. 480–494, Dec. 2017.

[8] H. Kamankesh, V. G. Agelidis, and A. Kavousi-Fard, "Optimal scheduling of renewable micro-grids considering plug-in hybrid electric vehicle charging demand," *Energy*, vol. 100, pp. 285–297, Apr. 2016.

[9] B. Zhao, H. Qiu, R. Qin, X. Zhang, W. Gu, and C. Wang, "Robust optimal dispatch of AC/DC hybrid microgrids considering generation and load uncertainties and energy storage loss," *IEEE Trans. Power Syst.*, vol. 33, no. 6, pp. 5945–5957, Nov. 2018.

[10] T. Niknam, R. Azizpanah-Abarghoee, and M. R. Narimani, "An efficient scenario-based stochastic programming framework for multi-objective optimal micro-grid operation," *Appl. Energy*, vol. 99, pp. 455–470, Nov. 2012.

[11] A. Papavasiliou and S. S. Oren, "Large-scale integration of deferrable demand and renewable energy sources," *IEEE Trans. Power Syst.*, vol. 29, no. 1, pp. 489–499, Jan. 2014.

[12] H. Liang and W. Zhuang, "Stochastic modeling and optimization in a microgrid: A survey," *Energies*, vol. 7, no. 4, pp. 2027–2050, 2014.

[13] A. Gholami, T. Shekari, F. Aminifar, and M. Shahidehpour, "Microgrid scheduling with uncertainty: The quest for resilience," *IEEE Trans. Smart Grid*, vol. 7, no. 6, pp. 2849–2858, Nov. 2016.

[14] M. H. Shams, M. Shahabi, and M. E. Khodayar, "Stochastic day-ahead scheduling of multiple energy carrier microgrids with demand response," *Energy*, vol. 155, pp. 326–338, Jul. 2018.

[15] C. Zhao and Y. Guan, "Unified stochastic and robust unit commitment," *IEEE Trans. Power Syst.*, vol. 28, no. 3, pp. 3353–3361, Aug. 2013.

[16] R. A. Gupta and N. K. Gupta, "A robust optimization based approach for microgrid operation in deregulated environment," *Energy Convers. Manage.*, vol. 93, pp. 121–131, Mar. 2015.

[17] C. Wang, B. Jiao, L. Guo, Z. Tian, J. Niu, and S. Li, "Robust scheduling of building energy system under uncertainty," *Appl. Energy*, vol. 167, pp. 366–376, Apr. 2016.

[18] D. Bertsimas, E. Litvinov, X. A. Sun, J. Zhao, and T. Zheng, "Adaptive robust optimization for the security constrained unit commitment problem," *IEEE Trans. Power Syst.*, vol. 28, no. 1, pp. 52–63, Feb. 2013.

[19] B. Zhang, Q. Li, L. Wang, and W. Feng, "Robust optimization for energy transactions in multi-microgrids under uncertainty," *Appl. Energy*, vol. 217, pp. 346–360, May 2018.

[20] H. Qiu, W. Gu, J. Pan, B. Xu, Y. Xu, M. Fan, and Z. Wu, "Multi-interval-uncertainty constrained robust dispatch for AC/DC hybrid microgrids with dynamic energy storage degradation," *Appl. Energy*, vol. 228, pp. 205–214, Oct. 2018.

[21] X. Lei, T. Huang, Y. Yang, Y. Fang, and P. Wang, "A bi-layer multi-time coordination method for optimal generation and reserve schedule and dispatch of a grid-connected microgrid," *IEEE Access*, vol. 7, pp. 44010–44020, 2019.

[22] Z. Bao, Q. Zhou, Z. Yang, Q. Yang, L. Xu, and T. Wu, "A multi time-scale and multi energy-type coordinated microgrid scheduling solution—Part I: Model and methodology," *IEEE Trans. Power Syst.*, vol. 30, no. 5, pp. 2257–2266, Sep. 2015.

[23] R. Palma-Behnke, C. Benavides, F. Lanas, B. Severino, L. Reyes, J. Llanos, and D. Saez, "A microgrid energy management system based on the rolling horizon strategy," *IEEE Trans. Smart Grid*, vol. 4, no. 2, pp. 996–1006, Jun. 2013.

- [24] Z. Li and Y. Xu, "Temporally-coordinated optimal operation of a multi-energy microgrid under diverse uncertainties," *Appl. Energy*, vol. 240, pp. 719–729, Apr. 2019.
- [25] C. Ju, P. Wang, L. Goel, and Y. Xu, "A two-layer energy management system for microgrids with hybrid energy storage considering degradation costs," *IEEE Trans. Smart Grid*, vol. 9, no. 6, pp. 6047–6057, Nov. 2018.
- [26] L. Wang, X. Han, C. Ren, Y. Yang, and P. Wang, "A modified one-cycle-control-based active power filter for harmonic compensation," *IEEE Trans. Ind. Electron.*, vol. 65, no. 1, pp. 738–748, Jan. 2018.
- [27] C. Ren, X. Han, L. Wang, Y. Yang, W. Qin, and P. Wang, "High-performance three-phase PWM converter with a reduced DC-link capacitor under unbalanced AC voltage conditions," *IEEE Trans. Ind. Electron.*, vol. 65, no. 2, pp. 1041–1050, Feb. 2018.
- [28] X. Liu, P. Wang, and P. C. Loh, "A hybrid AC/DC microgrid and its coordination control," *IEEE Trans. Smart Grid*, vol. 2, no. 2, pp. 278–286, Jun. 2011.
- [29] B. Papari, C. S. Edrington, I. Bhattacharya, and G. Radman, "Effective energy management of hybrid AC–DC microgrids with storage devices," *IEEE Trans. Smart Grid*, vol. 10, no. 1, pp. 193–203, Jan. 2019.
- [30] H. Qiu, B. Zhao, W. Gu, and R. Bo, "Bi-level two-stage robust optimal scheduling for AC/DC hybrid multi-microgrids," *IEEE Trans. Smart Grid*, vol. 9, no. 5, pp. 5455–5466, Sep. 2018.
- [31] M. Hosseinzadeh and F. R. Salmasi, "Robust optimal power management system for a hybrid AC/DC micro-grid," *IEEE Trans. Sustain. Energy*, vol. 6, no. 3, pp. 675–687, Jul. 2015.
- [32] N. Kinhekar, N. P. Padhy, F. Li, and H. O. Gupta, "Utility oriented demand side management using smart AC and micro DC grid cooperative," *IEEE Trans. Power Syst.*, vol. 31, no. 2, pp. 1151–1160, Mar. 2016.
- [33] D. Wang, S. Ge, H. Jia, C. Wang, Y. Zhou, N. Lu, and X. Kong, "A demand response and battery storage coordination algorithm for providing microgrid tie-line smoothing services," *IEEE Trans. Sustain. Energy*, vol. 5, no. 2, pp. 476–486, Apr. 2014.
- [34] A. Hussain, V.-H. Bui, and H.-M. Kim, "Robust optimal operation of AC/DC hybrid microgrids under market price uncertainties," *IEEE Access*, vol. 6, pp. 2654–2667, 2018.
- [35] F. Hong, R. Shan, H. Wang, and Y. Yan, "Analysis and calculation of inverter power loss," *Proc. CSEE*, vol. 28, no. 15, pp. 72–78, 2008.
- [36] A. D. Rajapakse, A. M. Gole, and P. L. Wilson, "Electromagnetic transients simulation models for accurate representation of switching losses and thermal performance in power electronic systems," *IEEE Trans. Power Del.*, vol. 20, no. 1, pp. 319–327, Jan. 2005.
- [37] C. Tian, C. Zhang, K. Li, and J. Wang, "Composite energy storage technology with compressed air energy storage in microgrid and its cost analysis," *Autom. Electr. Power Syst.*, vol. 39, no. 10, pp. 36–41, 2015.
- [38] B. Zhao, X. Zhang, J. Chen, C. Wang, and L. Guo, "Operation optimization of standalone microgrids considering lifetime characteristics of battery energy storage system," *IEEE Trans. Sustain. Energy*, vol. 4, no. 4, pp. 934–943, Oct. 2013.
- [39] H. Wang, Z. Lei, X. Zhang, B. Zhou, and J. Peng, "A review of deep learning for renewable energy forecasting," *Energy Convers. Manage.*, vol. 198, Oct. 2019, Art. no. 111799.
- [40] Y. He, Y. Qin, X. Lei, and N. Feng, "A study on short-term power load probability density forecasting considering wind power effects," *Int. J. Elect. Power Energy Syst.*, vol. 113, pp. 502–514, Dec. 2019.
- [41] T. Niknam, M. Zare, and J. Aghaei, "Scenario-based multiobjective Volt/Var control in distribution networks including renewable energy sources," *IEEE Trans. Power Del.*, vol. 27, no. 4, pp. 2004–2019, Oct. 2012.



XIAOQING HAN (Member, IEEE) received the B.Sc., M.Sc., and Ph.D. degrees from the College of Electrical and Power Engineering, Taiyuan University of Technology, Taiyuan, China.

She is currently a Professor with the Taiyuan University of Technology. Her research interests include power system simulation, stability analysis, and integration of renewable sources.



PENG WANG (Fellow, IEEE) received the Ph.D. degree from the University of Saskatchewan, Saskatoon, SK, Canada, in 1995 and 1998, respectively.

He is currently a Professor with the Electrical and Electronic Engineering School, Nanyang Technological University, Singapore. His research interests include power system planning and operation, renewable energy planning, electricity conversion systems, power market, and power system reliability analysis.



HAO YU received the B.S. degree in electrical engineering and automation from the Taiyuan University of Technology, Taiyuan, China, in 2017. He is currently pursuing the master's degree in the department of Electrical Engineering with School of Electrical and Power Engineering, Taiyuan University of Technology.

His current research interests include optimization techniques and microgrid economic dispatch.



WEN LI was born in Shanxi, China, in 1993. She received the B.S. degree in electrical engineering and automation from North China Electric Power University, Baoding, China, in 2014. She is currently pursuing the master's degree in Electrical Engineering with the Taiyuan University of Technology, Taiyuan, China.

Her current research interests include optimization techniques and power forecast in microgrid.



BIN WEI (Member, IEEE) received the B.S. and M.Sc. degrees in control science and engineering from Yanshan University, Qinhuangdao, China, in 2011 and 2015, respectively. He is currently pursuing the Ph.D. degree with the Department of Electrical Engineering, School of Electrical and Power Engineering, Taiyuan University of Technology, Taiyuan, China.

His current research interests include renewable energy generation forecast, microgrid modeling, sizing, and energy management.



LINGJUAN GUO was born in Shanxi, China, in 1995. She received the B.S. degree in electrical engineering and automation from the Taiyuan University of Technology, Shanxi, in 2017, where she is currently pursuing the master's degree in electrical engineering.

Her current research interests in energy storage system sizing in microgrid.

...